Optimization of gas diffusion media for elevated temperature polymer electrolyte fuel cells

Puneet K. Sinha[a,*], Chao-Yang Wang[a], Ay Su[b]

[a]*Electrochemical Engine Center (ECEC), Department of Mechanical and Nuclear Engineering, The Pennsylvania State University, University Park, PA 16802, USA*
[b]*Fuel Cell Center, Yuan-Ze University, Yuandong Road 135, Jhongli City, Taoyuan County 320, Taiwan*

Abstract

Elevated temperature operation (above $80\,^\circ C$) of polymer electrolyte fuel cell (PEFC) is characterized by more difficult membrane hydration and low availability of oxygen to the cathode catalyst layer. Better membrane hydration and less resistance to oxygen transport are required for improved performance of PEFC, operated at elevated temperatures. Hence, diffusion media, being a gateway for reactant and product water transport between the gas channel and catalyst layer, require optimization to ensure an improved PEFC performance at elevated temperatures. In the present study, a functional dependence of cell voltage on diffusion media properties is characterized and a two-dimensional single-phase, non-isothermal model is used to study the effect of diffusion media properties on the performance of fuel cell operated at $95\,^\circ C$. It was found that there exists an optimum value of effective diffusive length of diffusion media that provides peak performance. In addition, a functionally graded diffusion media design is proposed that provides a better performance than conventional diffusion media at elevated temperature operation.
© 2006 International Association for Hydrogen Energy. Published by Elsevier Ltd. All rights reserved.

Keywords: Polymer electrolyte fuel cell; Elevated temperature operation; Diffusion media optimization; Functionally graded diffusion media

1. Introduction

Low inlet relative humidity (RH) and elevated temperature (higher than $80\,^\circ C$) operations suit best to vehicular application as it enhances heat dissipation capability of a fuel cell stack and tolerance to minute amounts of carbon monoxide present in the fuel stream. Sinha et al. [1] investigated the performance of PEFC operated at $95\,^\circ C$ and low inlet humidity conditions. They identified better oxygen reduction reaction (ORR) kinetics, low membrane hydration and dominant oxygen depletion as the main characteristics of high temperature operation. They showed that towards the outlet oxygen depletion becomes dominant even before the membrane gets fully humidified. This behavior is in contrast to that of $80\,^\circ C$ operation where low inlet RH operations are dominated by membrane hydration but oxygen depletion governs the performance when the membrane becomes fully hydrated. An improved performance at elevated temperatures can be ensured by better membrane hydration and better oxygen availability to active sites in the cathode catalyst layer. Hence, diffusion media, being a gateway for reactant and product water transport between gas channel and catalyst layer, must be optimized such that it not only resist water transport from the catalyst layer to gas channel but also provides less resistance to oxygen transport from the gas channel to the cathode catalyst layer.

In the present paper we aim to portray the impact of diffusion media properties on the performance of elevated temperature PEFCs. First, a parametric study is carried out to investigate the effect of conventional diffusion media properties on the PEFC performance operated at $95\,^\circ C$. Then, a novel design of diffusion media is proposed that can provide better performance than conventional diffusion media.

2. Diffusion media characterization

In the macroscopic modeling framework, porosity, tortuosity and thickness of diffusion media are the main properties that

* Corresponding author. Tel.: +1814 865 9768; fax: +1814 863 4848.
  E-mail address: pks119@psu.edu (P.K. Sinha).

Nomenclature

a	water activity
C	molar concentration, $mol\,m^{-3}$
cgc	cathode gas channel
D	mass diffusivity of species, $m^2\,s^{-1}$
F	Faraday constant, $96487\,C\,mol^{-1}$
I	current density, $A\,m^{-2}$
j	transfer current, $A\,m^{-3}$
k	thermal conductivity, $W\,m^{-1}\,K^{-1}$
K	hydraulic permeability, m^2
p	pressure, Pa
n	number of electrons in electrochemical reaction
N	molar flow rate per unit membrane area, $mole\,m^{-2}\,s^{-1}$
n_d	electro-osmotic drag coefficient
R	the universal gas constant, $8.314\,J\,mol^{-1}\,K^{-1}$
RH	relative humidity
R_{dm}	resistance of diffusion media
s	stoichiometry coefficient in electrochemical reaction
S	source term in transport equation
T	temperature, K
$\boldsymbol{u}$	velocity vector, $m\,s^{-1}$
V_{cell}	cell potential, V
U_{oc}	thermodynamic equilibrium potential, V

Greek symbols

α	net water flux coefficient
α_a	transfer coefficient for anodic reaction
α_c	transfer coefficient for cathodic reaction
ε	volume fraction of gaseous phase in porous region
ε_{mc}	volume fraction of ionomer phase in catalyst layer
ϕ	phase potential, V
η	over potential, V
κ	ionic conductivity, S/m
λ	membrane water content, $mol\,H_2O/mol\,SO_3^-$
μ	fluid viscosity, $kg\,m^{-1}\,s^{-1}$
ρ	density, $kg\,m^{-3}$
ϕ	effective Diffusive Length, m

τ	viscous stress, $N\,m^{-2}$
ξ	stoichiometry flow ratio
δ	thickness, m
σ	electronic conductivity, $S\,m^{-1}$
τ	tortuosity of porous media

Subscripts

a	anode
an	anode
acl	anode catalyst layer
mean	average value
c	cathode
cath	cathode
cat	catalyst
ccl	cathode catalyst layer
dm	diffusion media
e	electrolyte
g	gas phase
GDL	gas diffusion layer
H_2	hydrogen
i	regions index
mem	membrane
MPL	micro porous layer
k	species index
O_2	oxygen
react	electrochemical reaction
ref	reference value
s	electronic
sat	saturation value
T	energy equation
u	momentum equation
w	water
Φ	potential equation
0	standard condition, 298.15 K and 101.3 kPa (1 atm)

Superscripts

e	electrolyte
eff	effective value in porous region

affect the performance of a PEFC. In this section, we present a one-dimensional analytical model to relate the performance of a PEFC with these diffusion media properties. The considered domain is sketched in Fig. 1. In the present analysis, catalyst layers are treated as interfaces between membrane and diffusion media. At a specified current density, I, the cell voltage, V_{cell}, is given by

$$V_{cell} = U_{oc} - \eta_{act} - \eta_{ohm} - \eta_{conc}, \tag{1}$$

where U_{oc} is the open circuit potential, η_{act}, η_{ohm} and η_{conc} the activation, ohmic and concentration overpotential, respectively. The Butler–Volmer equation can be expressed in the following form to separate activation and concentration overpotential:

$$\eta = \frac{RT}{\alpha_c F} \ln\left(\frac{I}{a i_o \delta_{cl}}\right) + \frac{RT}{\alpha_c F} \ln\left(\frac{C_{O_2,ref}}{C_{O_2,cat}}\right). \tag{2}$$

The first and second term on the right-hand side of Eq. (2) represents activation and concentration overpotential, respectively.
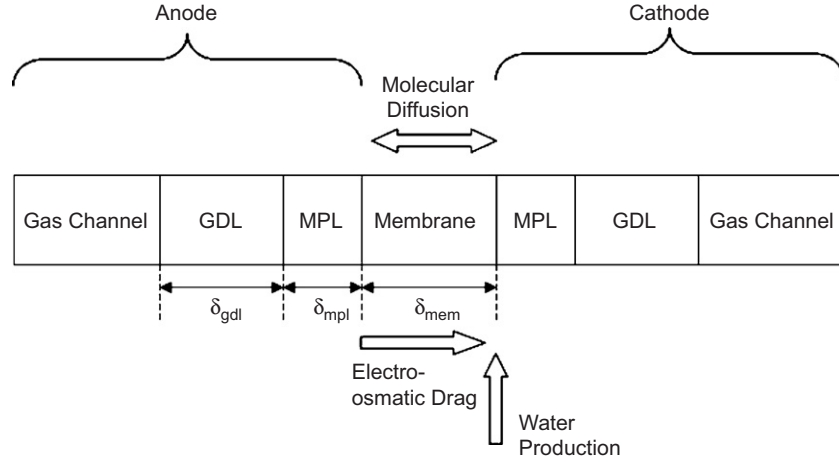
Fig. 1. One-dimensional control volume and transport processes for the analysis of voltage dependence on diffusion media properties. The catalyst layer is assumed to an interface between the membrane and MPL.

Hence the cell voltage can be expressed as

$$V_{\text{cell}} = U_{\text{oc}} - \frac{RT}{\alpha_c F} \ln\left(\frac{I}{ai_o \delta_{\text{cl}}}\right)$$

$$- \frac{RT}{\alpha_c F} \ln\left(\frac{C_{O_2,\text{ref}}}{C_{O_2,\text{cat}}}\right) - \frac{I\delta_{\text{mem}}}{\kappa_{\text{mem}}}. \tag{3}$$

In the present analysis, it is assumed that only the membrane contributes to the ohmic overpotential. The oxygen concentration in the catalyst layer, $C_{O_2,\text{cat}}$, is governed by Fick's diffusion law and can be related to diffusion medium properties as follows:

$$N_{O_2} = \frac{I}{4F} = \frac{C_{O_2,\text{gc}} - C_{O_2,\text{cat}}}{R_{\text{dm},O_2}}.$$

Hence,

$$\frac{C_{O_2,\text{ref}}}{C_{O_2,\text{cat}}} = \frac{C_{O_2,\text{ref}}}{C_{O_2,\text{gc}} - \dfrac{I}{4F} R_{\text{dm},O_2}}, \tag{4}$$

where N_{O_2} is the molar flow rate of oxygen through diffusion media and R_{dm,O_2} the resistance provided by diffusion media to oxygen transport. Oxygen concentration in the gas channel, $C_{O_2,\text{gc}}$, is solely governed by inlet conditions. Similarly, water concentration in the cathode catalyst layer, $C_{w,\text{ccl}}$, and hence water activity, a_{ccl}, can be expressed as follows:

$$\frac{I}{2F}(1 + \alpha) = \left(\frac{C_{w,\text{ccl}} - C_{w,\text{cgc}}}{R_{\text{dm},w,\text{cath}}}\right)$$

so,

$$C_{w,\text{ccl}} = C_{w,\text{cgc}} + \frac{I}{2F}(1 + \alpha) R_{\text{dm},w,\text{cath}} \tag{5}$$

and

$$a_{\text{ccl}} = RH_{\text{cgc}} + \frac{I}{2F}(1 + \alpha) \frac{R_{\text{dm},w,\text{cath}}}{C_{\text{sat,cath}}}, \tag{6}$$

where RH_{cgc} is the RH in the cathode gas channel, $R_{\text{dm},w,\text{cath}}$ the diffusive resistance to water transport through cathode

diffusion media, $C_{\text{sat,cath}}$ the water vapor saturation concentration on cathode side and function of temperature only, α the net water flux coefficient from the anode to the cathode catalyst layer. Similarly the water concentration in the anode catalyst layer, $C_{w,\text{acl}}$, and hence water activity, a_{acl}, is given by

$$C_{w,\text{acl}} = C_{w,\text{agc}} - \frac{I}{2F} \alpha R_{\text{dm},w,\text{an}}, \tag{7}$$

$$a_{\text{acl}} = RH_{\text{agc}} - \frac{I}{2F} \alpha \frac{R_{\text{dm},w,\text{an}}}{C_{\text{sat,an}}}, \tag{8}$$

where RH_{agc} and $R_{\text{dm},w,\text{an}}$ represents RH in the anode gas channel and diffusive resistance to water transport through anode diffusion media, respectively. The membrane water activity, a_{mem}, can be presumed to be an average of water activity in the anode and the cathode catalyst layer, a_{acl} and a_{ccl}, respectively, and hence is given by

$$a_{\text{mem}} = RH_{\text{mean}} + \frac{I}{2F}\left(\frac{(1 + \alpha) R_{\text{dm},w,\text{cath}}}{C_{\text{sat,cath}}} - \alpha \frac{R_{\text{dm},w,\text{an}}}{C_{\text{sat,an}}}\right), \tag{9}$$

where

$$RH_{\text{mean}} = \frac{RH_{\text{agc}} + RH_{\text{cgc}}}{2}. \tag{10}$$

In the present analysis, diffusion media consist of a macro gas diffusion layer, more commonly known as gas diffusion layer (GDL), and a micro gas diffusion layer, more commonly known as micro porous layer (MPL). So the total diffusive resistance to water transport can be expressed as

$$R_{\text{dm},w} = R_{\text{gdl},w} + R_{\text{mpl},w},$$

$$R_{\text{dm},w} = \left(\frac{\delta_{\text{gdl}} \tau_{\text{gdl}}}{\varepsilon_{\text{gdl}}} + \frac{\delta_{\text{mpl}} \tau_{\text{mpl}}}{\varepsilon_{\text{mpl}}}\right) \frac{1}{D_w}, \tag{11}$$

where D_w is the water vapor diffusion coefficient in gas channel, ε, τ and δ the porosity, tortuosity and thickness of the diffusion media (GDL and MPL), respectively. Subscript 'gdl' and

'mpl' represents GDL and micro porous layer, respectively. Using Eq. (11) for total diffusive resistance to water transport on anode and cathode side under the assumption that water vapor saturation concentration on anode and cathode is same and equal to C_{sat}, the membrane water activity, a_{mem}, can be written as

$$a_{mem} = RH_{mean} + \frac{I}{2FC_{sat}} \left(\frac{(1+\alpha)\varphi_{cath}}{D_{w,cath}} - \frac{\alpha\varphi_{an}}{D_{w,an}} \right), \quad (12)$$

where subscripts 'cath' and 'an' represents cathode and anode side, respectively. φ denotes the effective diffusive length and is given by

$$\varphi = \frac{\delta_{gdl}\tau_{gdl}}{\varepsilon_{gdl}} + \frac{\delta_{mpl}\tau_{mpl}}{\varepsilon_{mpl}}. \quad (13)$$

The proton conductivity of membrane is a function of membrane water content, which in turn depends on the membrane water activity. So from Eq. (12) the proton conductivity of membrane, κ_{mem}, can be expressed as

$$\kappa_{mem} = g(\varphi_{cath}, \varphi_{an}), \quad (14)$$

where $g(\phi_{cath}, \phi_{an})$ is a nonlinear function. Similarly, the total diffusive resistance to oxygen transport, R_{dm,O_2}, can be expressed as

$$R_{dm,O_2} = \left(\frac{\delta_{gdl}\tau_{gdl}}{\varepsilon_{gdl}} + \frac{\delta_{mpl}\tau_{mpl}}{\varepsilon_{mpl}} \right) \frac{1}{D_{O_2}} = \frac{\varphi_{cath}}{D_{O_2}}. \quad (15)$$

Combining the above equations, V_{cell} can be written as a function of diffusion media properties

$$V_{cell} = U_{oc} - \frac{RT}{\alpha_c F} \ln \left(\frac{I}{ai_o \delta_{cl}} \right) - \frac{I\delta_{mem}}{g(\varphi_{cath}, \varphi_{an})}$$

$$- \frac{RT}{\alpha_c F} \ln \left(\frac{C_{O_2,ref}}{C_{O_2,gc} - \frac{I\varphi_{cath}}{4FD_{O_2}}} \right). \quad (16)$$

As shown from Eq. (16), cell voltage is dependent on the effective diffusive length of diffusion media. Moreover, the functional dependence given in Eq. (16) shows that any combination of diffusion media thickness, porosity and tortuosity resulting in the same value of effective diffusion length will affect the cell voltage by the same magnitude.

3. Numerical model

A two-dimensional, non-isothermal, electrochemical and transport fully coupled PEFC model is developed based on the previous work of Um et al. [2], Meng et al. [3] and Ju et al. [4]. The complete set of conservation equations of mass, momentum, species, energy and charge (both protons and electrons) are solved with proper account of electrochemical kinetics in through-plane and flow direction. The model considers all nine-sub regions of PEFC: gas channels, macro and micro gas diffusion layers, catalyst layers and the membrane. Conservation equations of mass, momentum, species, proton electron and energy, are presented in Table 1. A detailed description of the governing equations and boundary conditions has been presented in previous papers [1–4] and thus not repeated here. Various functional relationships used for modeling are summarized in Table 2. The relevant cell design parameters are presented in Table 3 and all the properties used in the simulations are listed in Table 4.

The PEFC model is implemented into a commercial computational fluid dynamics package, STAR-CD, based on its user-defined capability [10]. Based on grid independence study of Meng et al. [11], 84 grid points in the through-plane direction and 112 in the flow direction are used. As mentioned in the previous section, cell voltage depends on the effective diffusive length of diffusion media. For the present work, the effect of effective diffusive length of diffusion media, φ, on the cell performance is studied by varying the tortuosity of diffusion media while keeping the porosity and the thickness of diffusion media the same.

Table 1
Single Phase non-isothermal PEFC model: governing equations with source terms

Conservation equations		Source terms
Mass	$\nabla \cdot (\rho\vec{u}) = 0$	
Momentum	$\frac{1}{\varepsilon^2}\nabla \cdot (\rho\vec{u}\vec{u}) = -\nabla p + \nabla \cdot \tau + S_u$	In diffusion and catalyst layers $S_u = -\frac{\mu}{K}\vec{u}$
Species	$\nabla \cdot (\vec{u}C_k) = \nabla \cdot (D_k^{eff}\nabla C_k) + S_k$	In catalyst layers $S_k = -\frac{S_k j}{nF}$
		For water in catalyst layers $S_k = -\nabla \cdot \left(\frac{n_d}{F}I \right) - \frac{S_k j}{nF}$
Proton	$\nabla \cdot (\kappa^{eff}\nabla\Phi_e) + S_\Phi = 0$	In catalyst layers $S_\Phi = j$
Electron	$\nabla \cdot (\sigma_s^{eff}\nabla\Phi_s) + S_\Phi = 0$	In catalyst layers $S_\Phi = -j$
Energy	$\nabla \cdot (\rho c_p \vec{u}T) = \nabla \cdot (k^{eff}\nabla T) + S_T$	In catalyst layers $S_T = j\left(\eta + T\frac{dU_o}{dT} \right) + \frac{I^2}{\kappa^{eff}}$
		In membrane $S_T = \frac{I^2}{\kappa^{eff}}$,
	Electrochemical reaction $\sum_k S_k M_k^z = ne^-$	where $\begin{cases} M_k \equiv \text{chemical formula of species } k \\ S_k \equiv \text{stoichiometry coefficient} \\ n \equiv \text{number of electrons transferred} \end{cases}$
Hydrogen oxidation reaction (HOR) in anode side		$H_2 - 2H^+ = 2e^-$
Oxygen reduction reaction (ORR) in cathode side		$2H_2O - O_2 - 4H^+ = 4e^-$

Table 2
Constitutive relationships used in the model

Quantity	Functional relationship	Reference
ORR kinetics	$ai_{0,c}^{ref}(T) = ai_{0,c}^{ref}(353\,K)\exp\left[-9000\left(\dfrac{1}{T} - \dfrac{1}{353.15}\right)\right]$	Parthasarathy et al. [5]
Diffusivity of gases in channels	$D_k = D_0\left(\dfrac{T}{T_0}\right)^{3/2}\left(\dfrac{P_0}{P}\right)$ for gas channel	Bird et al. [6]
Water content in membrane	$\lambda = \begin{cases} 0.043 + 17.81a - 39.85a^2 + 36.0a^3 & \text{for } 0 < a \leqslant 1 \\ 14 + 1.4(a-1) & \text{for } 1 < a \leqslant 3 \end{cases}$	Springer et al. [7]
Ionic conductivity of Nafion membrane	$\kappa_{mem} = (0.5139\lambda - 0.326)\exp\left[1268\left(\dfrac{1}{303} - \dfrac{1}{T}\right)\right]$	Springer et al. [7]
Ionic conductivity of Gore-select® membrane	$\kappa_{mem}^{eff} = \dfrac{1}{2}\cdot\kappa_{mem} = \dfrac{1}{2}\cdot(0.5139\lambda - 0.326)\exp\left[1268\left(\dfrac{1}{303} - \dfrac{1}{T}\right)\right]$	Ju et al. [8]
Water diffusivity in Nafion membrane	$D_{w,mem} = \begin{cases} 2.692661843 \times 10^{-10} & \text{for } \lambda \leqslant 2 \\ \{0.87(3-\lambda) + 2.95(\lambda-2)\} \times 10^{-10}\cdot e^{(7.9728-(2416/T))} & \text{for } 2 < \lambda \leqslant 3 \\ \{2.95(4-\lambda) + 1.642454(\lambda-3)\} \times 10^{-10}\cdot e^{(7.9728-(2416/T))} & \text{for } 3 < \lambda \leqslant 4 \\ (2.563 - 0.33\lambda + 0.0264\lambda^2 - 0.000671\lambda^3) \times 10^{-10}\cdot e^{(7.9728-(2416/T))} & \text{for } \lambda > 4 \end{cases}$	Springer et al. [7]
Water diffusivity in Gore-select® membrane	$D_{w,mem}^{eff} = \frac{1}{2}D_{w,mem}$	Ju et al. [8]
Electro-osmotic drag	$n_d = 1$	Zawodzinski et al. [9]

Table 3
Cell design parameters

Description	Value
Anode/cathode macro gas diffusion layer thickness	0.230 mm
Anode/cathode micro gas diffusion layer thickness	0.060 mm
Anode/cathode catalyst layer thickness	0.010 mm
Anode/cathode gas channel depth	0.846 mm
Height of cell in the in-plane direction	0.686 mm
Membrane width (Gore-select®)	0.018 mm
Porosity of anode/cathode macro gas diffusion layer, ε_{GDL}	0.7
Porosity of anode/cathode micro gas diffusion layer, ε_{MPL}	0.5
Porosity of anode/cathode catalyst layer, ε_{cat}	0.6
Volume fraction of ionomer in anode/cathode catalyst layer, ε_{mc}	0.26
Permeability of anode/cathode macro gas diffusion layer, K_{GDL}	$4.0 \times 10^{-12}\,m^2$
Permeability of anode/cathode micro gas diffusion layer, K_{MPL}	$2.0 \times 10^{-15}\,m^2$
Operating pressure at both anode and cathode side	270 KPa
Stoichiometry at both anode and cathode inlet	30%
Average current density	1.6 A cm^{-2}
Flow configuration	Co-flow

4. Results and discussion

As mentioned in previous section, the porosity, thickness and tortuosity, which in turn depend on detailed microstructure of diffusion media, should be engineered to ensure a better water retention in membrane and better availability of oxygen to the active sites in cathode catalyst layer. In Section 2, it was shown that these three properties, however independent, affect the cell performance via effective diffusion length, φ, given by Eq. (13). Thus, any set of values for porosity, thickness and tortuosity of diffusion media that provides same value of effective diffusive length will affect the cell performance by same magnitude. This conclusion significantly reduces the efforts required to optimize diffusion media structure. In the present work, the effect of effective diffusive length on cell performance is investigated only by varying tortuosity while keeping porosity and thickness of diffusion media same.

4.1. Effect of diffusion media properties

A parametric study is carried out for various tortuosity values of diffusion media for 1.6 A/cm² average current density operation with 30% inlet RH at both anode and cathode inlets. The predicted cell voltage as a function of the effective diffusive length is listed in Table 5. As shown in Table 5, with increase in the effective diffusive length, the cell voltage increases to a maximum value but further increase in the effective diffusive length drastically decreases the cell voltage.

Fig. 2 shows the variation of current density in the middle section of membrane along the flow direction for various tortuosity values. In Fig. 2 notation 'tau2' denotes a diffusion media with a tortuosity value of 2 and likewise. As shown in Fig. 2, near the inlet section, current density decreases along the flow direction because of water transport from anode to cathode catalyst layer due to electro osmotic drag [1]. A more tortuous diffusion media provide more resistance to water transport hence

Table 4
Kinetic, physical, transport and thermal properties

Description	Reference	Values
Exchange current density×specific reaction surface in anode side, $ai_{0,a}^{ref}$	Ju et al. [8]	$1.0 \times 10^9 \, A \, m^{-3}$
Exchange current density×specific reaction surface in cathode side, $ai_{0,c}^{ref}$	Sinha et al. [1]	$2.0 \times 10^4 \, A \, m^{-3}$
Reference hydrogen molar concentration, $C_{H_2,ref}$	Ju et al. [8]	$40.88 \, mol \, m^{-3}$
Reference oxygen molar concentration, $C_{O_2,ref}$	Ju et al. [8]	$40.88 \, mol \, m^{-3}$
Anodic and cathodic transfer coefficients for hydrogen oxidation reaction		$\alpha_a = \alpha_c = 1$
Cathodic transfer coefficient for oxygen reduction reaction		$\alpha_c = 1$
Dry membrane density, $\rho_{dry,mem}$	Courtsey to Gore	$2000 \, kg \, m^{-3}$
Equivalent weight of membrane, EW	Courtesy to Gore	$1.1 \, kg \, mol^{-1}$
Faraday constant, F		$96487 \, C \, mol^{-1}$
H_2 diffusivity in the anode gas channel, $D_{0,H_2,a}$	Bird et al. [6]	$1.1028 \times 10^{-4} \, m^2 \, s^{-1}$
H_2O diffusivity in the anode gas channel, $D_{0,w,a}$	Bird et al. [6]	$1.1028 \times 10^{-4} \, m^2 \, s^{-1}$
O_2 diffusivity in the cathode gas channel, $D_{0,O_2,c}$	Bird et al. [6]	$3.2348 \times 10^{-5} \, m^2 \, s^{-1}$
H_2O diffusivity in the cathode gas channel, $D_{0,w,c}$	Bird et al. [6]	$7.35 \times 10^{-5} \, m^2 \, s^{-1}$
Thermal conductivity of hydrogen (H_2), k_{H_2}	Bird et al. [6]	$0.2040 \, W \, m^{-1} \, K^{-1}$
Thermal conductivity of oxygen (O_2), k_{O_2}	Bird et al. [6]	$0.0296 \, W \, m^{-1} \, K^{-1}$
Thermal conductivity of water vapor, k_w	Bird et al. [6]	$0.0237 \, W \, m^{-1} \, K^{-1}$
Thermal conductivity of macro gas diffusion layer, k_{GDL}	Courtesy to Gore	$1.19 \, W \, m^{-1} \, K^{-1}$
Thermal conductivity of micro gas diffusion layer, k_{MPL}	Courtesy to Gore	$1.19 \, W \, m^{-1} \, K^{-1}$
Electronic conductivity of macro gas diffusion layer, σ_{GDL}	Courtesy to Gore	$6666.67 \, S \, m^{-1}$
Electronic conductivity of micro gas diffusion layer, σ_{MPL}	Courtesy to Gore	$200 \, S \, m^{-1}$
Electronic conductivity of catalyst layer, σ_{cat}	Courtesy to Gore	$200 \, S \, m^{-1}$
Electronic conductivity of bipolar plate, σ_{BP}	Courtesy to Gore	$20000 \, S \, m^{-1}$

Table 5
Cell voltage as a function of effective diffusive length of conventional diffusion media

τ_{GDL}/τ_{MPL}	Effective diffusive length (μm)	Cell voltage (V)
2/2	897.14	0.397
3/3	1345.71	0.422
4/4	1794.28	0.429
5/5	2242.85	0.434
6/6	2691.43	0.432
7/7	3140.0	0.393

higher water concentration at the membrane-cathode catalyst layer interface and results in more back diffusion of water from the cathode to the anode side of the membrane which in turn reduces the net water flux from the anode to the cathode side of the membrane. Thus, a more tortuous diffusion media provide less decrease in current density near the inlet of gas channel, as shown in Fig. 2. Current density increases along the flow direction due to water uptake. Towards the outlet of gas channel, oxygen depletion dominates membrane hydration and current density decreases along the flow direction. As shown in Fig. 2, peak current density shifts towards the left with increase in tortuosity. This denotes that the fraction of length over which oxygen depletion dominates over membrane hydration increases with tortuosity.

Fig. 3 shows the variations of ohmic and concentration overpotentials along the flow direction for different tortuosities of diffusion media. In the present work, it is assumed that only membrane contributes to the ohmic overpotential. In Fig. 3, 'eta ohmic' and 'eta conc' denotes ohmic overpotential and concentration overpotential, respectively. For clarity, overpoten-

tials are plotted for three tortuosity values. As shown in Fig. 3, ohmic overpotential decreases and concentration overpotential increases monotonically along the flow direction due to membrane hydration and oxygen depletion along the flow direction, respectively. Increase in tortuosity provides better membrane hydration. However, more tortuous diffusion medium provides more resistance to oxygen transport and results in large concentration overpotential. As tortuosity increases from 2 to 5, the decrease in ohmic overpotential is higher than the increase in concentration overpotential whereas, concentration overpotential increases very sharply as tortuosity increases from 5 to 7 as shown in Fig. 3. This results in a decrease in cell voltage as tortuosity increases beyond 5.

4.2. Functionally graded diffusion media

A better PEFC performance at 95 °C can be insured by a diffusion media, which provide better water retention and low resistance to oxygen transport especially towards the exit of gas channel. To meet this criterion we propose a functionally graded diffusion media, shown schematically in Fig. 4. As shown in Fig. 4, functionally graded diffusion media is composed of a 'fine' structure, a diffusion media with large tortuosity, and a 'coarse' structure, diffusion media with small tortuosity. The transition from fine to coarse structure occurs after a certain length along the flow direction. The coarse structure provides less resistance to oxygen transport and hence improves performance towards the outlet which was otherwise governed by oxygen depletion along the flow direction near the outlet of gas channel. However, coarse diffusion media also provide poor water retention hence a proper selection of transition length
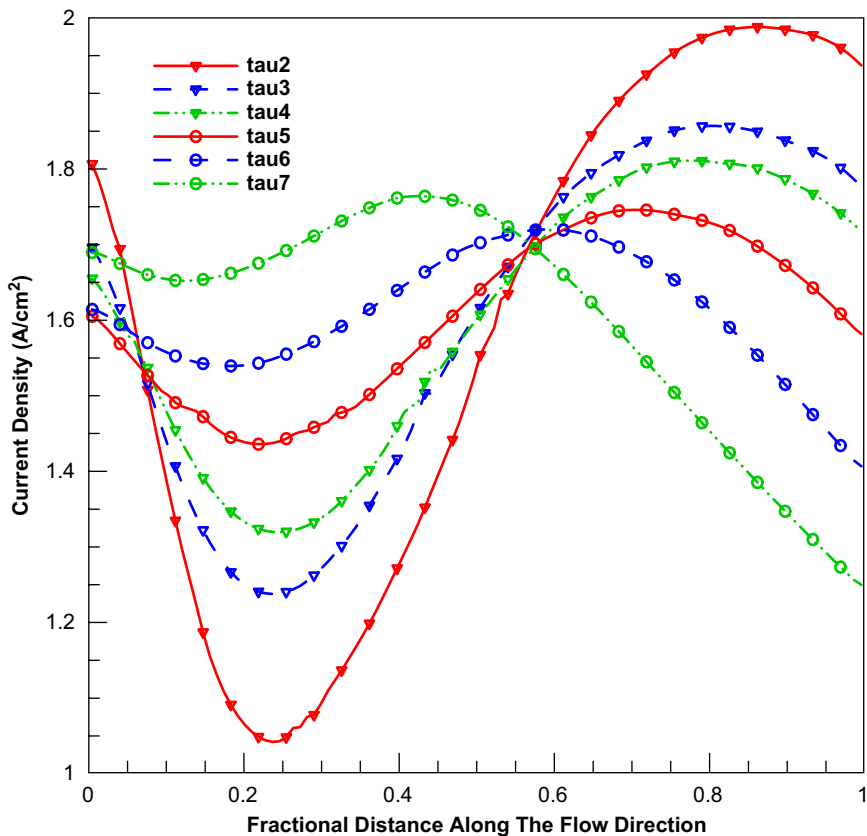
Fig. 2. Current density profiles along the flow direction in the middle section of membrane as function of diffusion media tortuosity for conventional diffusion media.
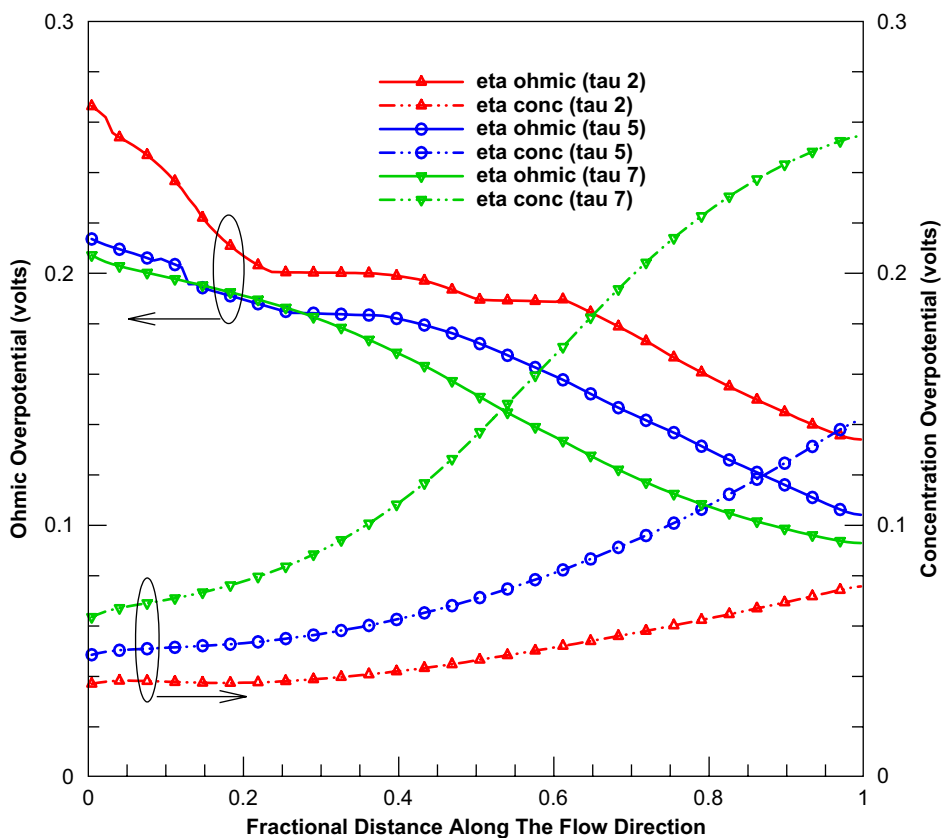
Fig. 3. Ohmic and concentration overpotential variation along the flow direction as function of diffusion media tortuosity for conventional diffusion media.
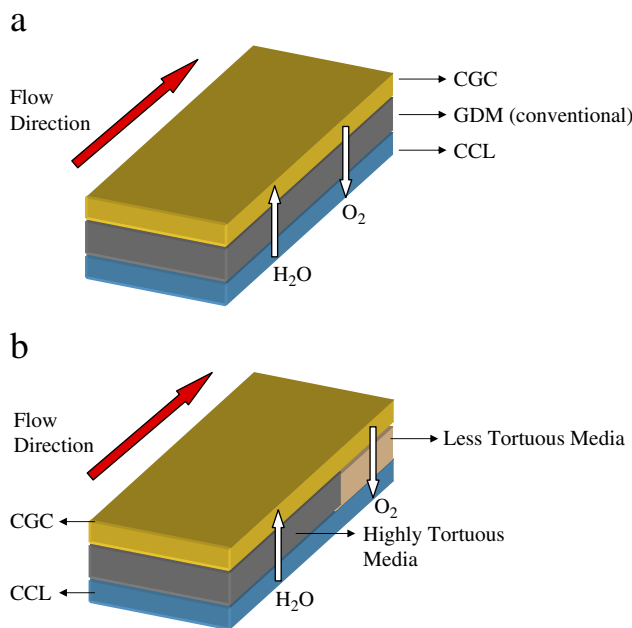
Fig. 4. Schematic representation of functionally graded diffusion media (b) and its comparison with conventional diffusion media (a).
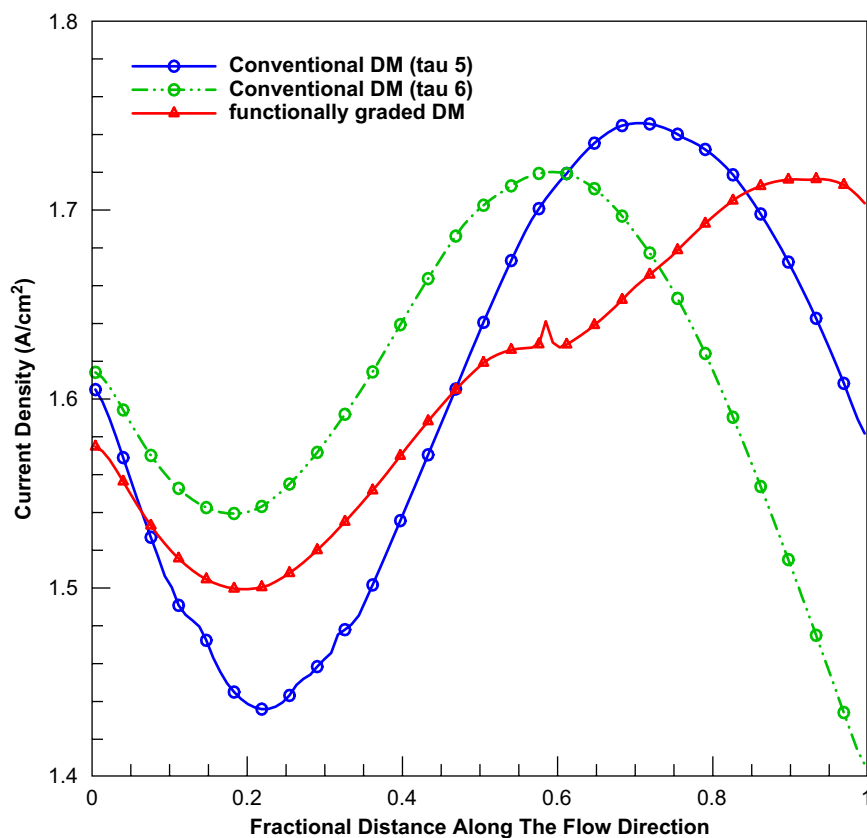
Fig. 5. Current density profiles along the flow direction in the middle section of membrane for conventional and functionally graded diffusion media.

(transition from fine to coarse diffusion media) is required to ensure an improved performance.

The current density profiles along the flow direction, as shown in Fig. 2, can be used to determine the transition length

e.g. for a diffusion media having tortuosity value of 6, oxygen concentration at the active sites in the cathode catalyst layer governs the cell performance for approximately 45% of the later half of the cell length. Hence, a functionally graded

Table 6
Cell voltage for conventional and functionally graded diffusion media

τ_{GDL}/τ_{MPL}	Type of diffusion media	Cell voltage (V)
5/5	Conventional diffusion media	0.434
6/6	Conventional diffusion media	0.432
(Fine: coarse) 6:3/6:3	Functionally Graded diffusion media	0.45

diffusion media can be composed of a fine structure with tortuosity value of 6 for 55% of the cell length from the inlet and a coarse structure for the rest 45% of the cell length. It should be noted that the selection of transition length is dependent on the inlet conditions and the average current density.

Fig. 5 shows the current density distribution along the flow direction for a functionally graded diffusion media. A functionally graded diffusion media with high tortuosity value of 6 and low tortuosity value of 3 is chosen for the present study. In order to clearly show the effect of functionally graded diffusion media, current density distributions for a conventional diffusion media with tortuosity value of 5 and 6 are also plotted. Tortuosity value of 5 corresponds to the maximum cell voltage with the conventional diffusion media, as shown in Table 5. As shown in Fig. 5, in contrast to the conventional diffusion media, towards the outlet of gas channel current density increases along the flow direction for functionally graded diffusion media. Low tortuosity of functionally diffusion media towards the outlet of gas channel provides less resistance to oxygen transport and causes membrane hydration to dominate over oxygen depletion along the flow direction. A nose shape in the current density profile for functionally graded diffusion media shows the transition from fine to coarse structure. The predicted cell voltage for the functionally graded diffusion media and the conventional diffusion media with tortuosity value of 5 and 6 are listed in Table 6. As shown in Table 6, the functionally graded diffusion media provides an additional 15 mV increase over the maximum voltage obtained with the conventional diffusion media.

5. Conclusions

PEFC performance depends on the effective diffusive length of diffusion media hence any combination of diffusion media thickness, porosity and tortuosity that will result in the same value of effective diffusion length will affect the cell voltage by the same magnitude. In the present study, the effect of effective diffusive length of diffusion media on PEFC performance was

investigated by varying the tortuosity of diffusion media while keeping the porosity and thickness the same. It was found that there exists an optimum value of effective diffusive length that provides maximum cell voltage.

In addition, a functionally graded diffusion media was proposed that provide a combination of better water retention near the inlet of gas channel and better oxygen concentration in the cathode catalyst layer towards the outlet of gas channel. It was found that a diffusion media composed of a structure having smaller effective diffusive length towards the outlet of gas channel poses less resistance to oxygen transport and thus, significantly changes the current density distribution along the flow direction. A better performance with the functionally graded diffusion media can be ensured by proper optimization of the fine (large effective diffusive length) and the coarse (small effective diffusive length) structure of the functionally graded diffusion media.

References

[1] Sinha PK, Wang CY, Beuscher U. Transport phenomena in elevated temperature polymer electrolyte fuel cells. J Electrochem Soc 2006, in press.

[2] Um S, Wang CY, Chen KS. Computational fluid dynamics modeling of proton exchange membrane fuel cells. J Electrochem Soc 2000;147: 4485–93.

[3] Meng H, Wang CY. Electron transport in PEFCs. J Electrochem Soc 2004;151:A358–67.

[4] Ju H, Meng H, Wang CY. A single-phase non-isothermal model for PEM fuel cells. Int J Heat Mass Transfer 2005;48:1303–5.

[5] Parthasarathy A, Srinivasan S, Appleby AJ. Temperature dependence of the electrode kinetics of oxygen reduction at the platinum/nafion® interface—a microelectrode investigation. J Electrochem Soc 1992;139:2530–7.

[6] Bird RB, Stewart WE, Lightfood EN. Transport phenomena. New York, NY: Wiley; 1960.

[7] Springer TE, Zawodizinski TA, Gottesfeld S. Polymer electrolyte fuel cell model. J Electrochem Soc 1991;136:2334–41.

[8] Ju H, Wang CY, Cleghorn S, Beuscher U. Non-isothermal modeling of polymer electrolyte fuel cells part I: experimental validation. J Electrochem Soc 2005;152:A1645–53.

[9] Zawodzinski TA, Davey J, Valerio J, Gottesfeld S. The water content dependence of electro-osmotic drag in proton-conducting polymer electrolytes. Electrochim Acta 1995;40:297–302.

[10] STAR-CD Version 3.15 Methodology, CD-Adapco Group; 2001.

[11] Meng H, Wang CY. Large-scale simulation of polymer electrolyte fuel cells by parallel computing. Chem Eng Sci 2004;59:A3331–43.